



# Enhancing extraction of proanthocyanidins from Chinese quince fruit by ball-milling and enzyme hydrolysis: yield, structure, and bioactivities

Wan-Qing KONG<sup>1</sup>, Ming-Wei LIU<sup>1</sup>, Shou-Tao WANG<sup>1</sup>, Hui-Hui GAO<sup>1</sup>, Zhao QIN<sup>1\*</sup> , Hua-Min LIU<sup>1</sup>,  
Xue-De WANG<sup>1\*</sup> , Jing-Ren HE<sup>2,3</sup>

## Abstract

Chinese quince fruits are rich in proanthocyanidins (PAs), which have antioxidant properties. This work describes a method to isolate PAs from Chinese quince fruits by a combination of ball-milling and enzyme hydrolysis pretreatments. The yield, total PA and total phenolic contents, structural characteristics, antioxidant activity, and  $\alpha$ -amylase inhibitory activity of different pretreated PA samples were determined and analyzed. Among them, the ball-milling combined with multi-enzyme (cellulase, xylanase, and pectinase) hydrolysis pretreated sample (BEP-4) was the most outstanding. The yield of BEP-4 could be improved up to 7.72%, which was 2.51 times higher than that of the conventional organic solvent extraction method (3.02%). It had the highest total phenols and PAs content of  $750.98 \pm 6.95$  and  $948.72 \pm 3.50$  mg/g extract, respectively. The thermal stability and molecular weight (9610 Da) of BEP-4 were lower than other fractions. BEP-4 contained a high proportion of PC structure (98.35%) and flavan-3-ol content (87.88%). It also had the highest antioxidant capacity with  $IC_{50}$  values of  $131.45 \pm 0.97$ ,  $22.66 \pm 0.32$ ,  $134.05 \pm 0.71$ , and  $182.07 \pm 0.28$   $\mu$ g/mL for DPPH, ABTS, hydroxyl radical scavenging capacity, and  $\alpha$ -amylase inhibiting capacity, respectively. These investigations provide a new, efficient way to isolate PAs from Chinese quince fruits, and reveal that Chinese quince fruits may be a good source of antioxidants, worthy of further development.

**Keywords:** Chinese quince; proanthocyanidins; characterization; enzymatic hydrolysis; ball-milling.

**Practical Application:** The combination of ball-milling and enzyme hydrolysis pretreatments can be used for the efficient extraction of PAs from Chinese quince fruits.

## 1 Introduction

The fruits of *Chaenomeles sinensis* (Thouin) Koehne, commonly known as Chinese quince, have traditionally been used as a source of medicine and food (Sawai-Kuroda et al., 2013). Chinese quince resources with a high annual yield up to 100,000 tons in Baihe County, Shaanxi Province alone (Qin et al., 2020); however, the overall utilization rate of Chinese quinces is not high due to their hardy and sour flesh, which is not directly edible. How to improve the overall utilization of the Chinese quince industry is a matter of concern. Previous papers have shown that Chinese quince fruits are rich in bioactive phenolic compounds. Among these phenolic compounds, proanthocyanidins (PAs) have the highest percentage, up to about 80% (Jiao et al., 2020).

PAs, are a group of natural phenolic compounds derived from flavan-3-ols monomers (catechin or epicatechin) (Lv et al., 2021), which are secondary metabolites in the synthesis of flavonoids (Wang et al., 2022). Currently, PAs are widely used in food, pharmaceutical and cosmetic applications due to their strong biological activities (Wojdyło et al., 2018). In recent years, as consumers are concerned about the safety of synthetic antioxidants, natural antioxidants have received close attention

due to their green and safe antioxidant effects, etc. Chinese quince PAs have strong antioxidant activity (Li et al., 2021), therefore, can be applied as an effective natural antioxidant to improve the added value and overall utilization of Chinese quince.

Based on their chemical structure, PAs are categorized as either free or insoluble-bound. Free PAs, which are not bound to cell wall major components, can be readily extracted by organic solvents (Fernandes et al., 2020); Insoluble-bound PAs, which have non-covalent bonds with cell wall components such as protein and pectin, and therefore typically need pretreatment before they can be extracted (Zeller, 2019). Compared with other fruits containing PAs, Chinese quince fruits have higher contents of bound PAs (up to 40% of total PAs) (Hamazu & Mizuno, 2014). In addition, some free PAs undergo some reactions with cell wall components to convert into bound PAs during the separation process (Waterlot et al., 2014). Conventional separation methods cannot effectively extract bound PAs. Therefore, a significant amount of bound PAs remains in the extraction residue, which leads to low overall separation efficiency. Therefore, there is a

Received 12 Aug., 2022

Accepted 19 Sept., 2022

<sup>1</sup>College of Food Science and Engineering & Institute of Special Oilseed Processing and Technology, Henan University of Technology, Zhengzhou, China

<sup>2</sup>National R&D Center for Se-rich Agricultural Products Processing, Hubei Engineering Research Center for Deep Processing of Green Se-rich Agricultural Products, School of Modern Industry for Selenium Science and Engineering, Wuhan Polytechnic University, Wuhan, China

<sup>3</sup>Key Laboratory for Deep Processing of Major Grain and Oil, Ministry of Education, Hubei Key Laboratory for Processing and Transformation of Agricultural Products, Wuhan Polytechnic University, Wuhan, China

\*Corresponding author: qinzhao505@163.com; wangxuede1962@126.com

need to find and develop methods for efficient isolation and extraction of PAs from Chinese quince.

Pretreatment can promote the release of bound PAs during extraction (Domínguez-Rodríguez et al., 2017), improving the overall separation and extraction efficiency of PAs from Chinese quince. Acid and alkali hydrolysis are the most common pretreatment methods. However, these traditional pretreatment methods require a strict pH environment, high processing temperature, and easy to affect the basic structure and composition of PAs. Enzymatic hydrolysis has the advantages of mild conditions, a high extraction rate, that is increasingly used as an alternative to traditional pretreatment techniques (Shahidi & Yeo, 2016). Enzyme-assisted extraction is based on the degradation of cell wall components, thereby liberating the bound PAs (Cascaes-Teles et al., 2021). Enzyme-assisted extraction is one of the methods to improve the extraction efficiency of PAs, as this method helps to obtain PAs attached to the plant cell walls, which are more difficult to obtain by conventional extraction methods (Silva et al., 2022). In addition, ball milling technology has been reported to be an efficient and environmentally friendly method for ultrafine grinding. Ball milling pretreatment can help break the bond between cell wall components and PAs and disrupt the cell wall structure. The disruption of the cell wall structure of Chinese quince can facilitate better enzyme action on the cell wall components and allow fuller contact between PAs and the extraction solvent. The low temperature used in the ball-milling treatment process can help avoid oxidation or transformation of PAs and ensure the stability of PA structures (Liu et al., 2017). Enzymatic extraction of PAs has been studied; however, the combination of ball-milling treatment and enzyme hydrolysis for the extraction of PAs has not been reported.

In this present study, an enhanced method for isolating PAs from Chinese quince fruits was developed; the method is a combination of ball-milling and enzyme-assisted extraction. Three enzymes (cellulase, xylanase, and pectinase,) and their blends were used. The yield, structure,  $\alpha$ -amylase inhibitory activity, and antioxidant activity of PAs obtained by ball-milling assisted enzymatic hydrolysis pretreatment were compared with those obtained by ball-mill pretreatment and conventional solvent extraction. This study provides a new extraction method for obtaining PAs from Chinese quince fruits, thereby laying the foundation for the potential applications of Chinese quince PAs as natural antioxidants in foods.

## 2 Materials and methods

### 2.1 Plant material and chemicals

Fresh Chinese quince fruits were obtained from a local plantation base (Zhengzhou, China). Chemicals and reagents were of analytical grade and purchased from Zhiyuan (Tianjin, China). Celluclast 1.5 L (700 EGU/g, endoglucanase units per gram), Pectinex XXL (10000 PECTU/mL, pectin transeliminase units per gram), and xylanase Shearzyme 500L (500 FXU-S/g, endo-1,4- $\beta$ -D-xylan hydrolases units per gram) were all obtained from Novozymes (Beijing, China).

### 2.2 Sample preparation

Chinese quinces were washed, seeded, sliced, then freeze-dried for 48 h, ground, and sieved by an 80-mesh sieve. The powder was defatted for 8 h at 50 °C with petroleum ether. The defatted dried Chinese quince powder was sealed and stored in a desiccator for later use. This powder, which had not been subjected to ball-milling, was defined as UMS.

### 2.3 Isolation and extraction of PAs

#### *Conventional organic solvent extraction*

Firstly, 10 g of UMS was soaked in a 400 mL solvent mixture of acetone: water: acetic acid (70: 29.5: 0.5, v/v/v). The mixture was magnetically stirred for 3 h, and centrifuged for 10 min at 4800 g to remove insoluble solids. The supernatant was recovered and concentrated under vacuum at 30 °C until the organic solvent was completely removed (Li et al., 2015a). The remaining fraction was freeze-dried and purified by AB-8 macroporous resin column and Sephadex LH-20, using a method described in a published paper (Qi et al., 2016); the resulting powder was named UMP.

#### *Organic solvent extraction after ball-milling*

The ball-milling process was run for 48 cycles by a Fritsch planetary ball mill (CTPT Co., Ltd., China). A single cycle comprised of milling for 10 min and pausing for 20 min. Briefly, two grinding tanks (volume of 500 mL) were each filled with 100 g UMS, and grinding balls (material: zirconia; size: 60 mm) were added in a 6:1 ratio of agate ball to sample (Yang et al., 2019a). The resulting powder was named BMS.

BMS was extracted with organic solvent and purified as described in section 2.3.1. The PA fraction obtained was named BMP.

#### *Organic solvent extraction after ball-milling and enzyme-assisted pretreatments*

Based on our previous study (Qin et al., 2018) with minor modifications, a sample buffer was obtained by adding 20 g of BMS to 250 mL of 0.2 M HAc-NaAc buffer (pH 4.7). Four sample buffers were prepared in this way. Then 2 mL cellulase (700 EGU/g) was added to the first one, 2 mL xylanase (500 U/g) was added to the second, 2 mL pectinase (10000 PECTU/mL) was added to the third, and multi-enzyme (2 mL cellulase, 2 mL xylanase, and 2 mL pectinase) was added to the fourth. The mixtures were reacted at 37 °C for 24 h, then centrifuged for 5 min at 4800 g. The insoluble residues after cellulase, xylanase, pectinase, and multi-enzyme hydrolysis pretreatments were labeled as BES-1, BES-2, BES-3, and BES-4, respectively. Then PAs were isolated from these four, using the conventional organic solvent extraction and purification method described in Section 2.3.1. The four PA fractions obtained from BES-1, BES-2, BES-3, and BES-4 were named BEP-1, BEP-2, BEP-3, and BEP-4, respectively.

## 2.4 Evaluation of bioactive compounds

### Total phenolic content (TPC)

The TPCs of the six purified samples were determined according to the previous study (Zhang et al., 2016). The TPC of each sample was recorded as milligrams of epicatechin (EC) per gram of extracts.

### Total PA content (TPA)

The TPAs of the six purified samples were measured according to a previous report (Lv et al., 2015). The TPA of each sample was recorded as mg proanthocyanidin B<sub>1</sub> equivalents (PB<sub>1</sub>)/g extracts.

### Extraction yield of PAs

The extraction yield of PAs was defined as follows (Equation 1):

$$\text{Yield (\%)} = \frac{\text{the weight of PAs (g)}}{\text{the weight of Chinese quince powder raw material (g)}} \times 100\% \quad (1)$$

## 2.5 X-ray diffraction (XRD) analysis

To determine the crystalline changes in the cell wall structure of Chinese quinces after each pretreatment, XRD analysis were performed with an XRD-6000 Xray diffractometer. The crystallinity index (CrI) was determined using the XRD spectra. Samples were scanned at a speed of 2°·min<sup>-1</sup> from 10° to 60°. The step size was set at 0.013°.

## 2.6 Scanning electron microscope (SEM) examination

Morphological characteristics of the cell wall structure of Chinese quinces after different pretreatments were studied by SEM. Samples were placed on stubs, and sputter coated. Samples were observed at 3.0 kV. The images were obtained at 1000× magnifications.

## 2.7 Fourier transform infrared spectroscopy (FT-IR) analysis

FT-IR spectra of the six purified samples were obtained on a Frontier FT-IR 115089 spectrometer to further verify their structures, using a KBr disk containing 1% finely ground samples. Thirty-two scans from 4000 to 400 cm<sup>-1</sup> in transmission mode were performed.

## 2.8 Gel permeation chromatography (GPC) analysis

GPC was performed using a Waters 1525 instrument with an RI Detector Waters 2414, with a flow rate of 1 mL/min at 25 °C for 15min. A standard calibration was created using standard polystyrene in a molecular weight range of 200-100000 Da. Before the determination, the six purified PA samples were subjected to acetylation according to a previous report (Roy et al., 2021).

## 2.9 Thermal analysis

The TGA spectra were acquired on a Q5000 TGA analyzer (TA Instruments, USA) in a nitrogen atmosphere (60 mL·min<sup>-1</sup>). 5 mg of each of the six purified PA samples was transferred to a platinum pan, and the data was recorded from 25 to 700 °C at a heating rate of 10 °C·min<sup>-1</sup>.

## 2.10 MALDI-TOF-MS analysis

The MALDI-TOF-MS spectra of the purified PA samples were acquired with a MALDI-TOF-MS instrument (Bruker Reflex III, Germany). Samples were irradiated at 337 nm with a pulsed nitrogen laser, and the duration of the laser pulse was 3 ns. The analytical parameters were done according to a previous report (Esquivel-Alvarado et al., 2021).

## 2.11 LC-MS/MS analysis

The monomers in the oligomers and homopolymers in the purified PA extracts were detected using an LC-MS/MS method as previously reported (Fraser et al., 2016).

## 2.12 Nuclear magnetic resonance (NMR) analysis

The heteronuclear single quantum coherence (HSQC) spectra of the purified PA samples were recorded on a Bruker Avance III HD 500 MHz NMR spectrometer (Bruker Instruments, Inc., Switzerland). 50 mg of sample was dissolved in 0.5 mL of CD<sub>3</sub>OD and put in a 5 mm NMR tube. The 2D-HSQC NMR experiment was carried out according to the previous report (Huang et al., 2015).

## 2.13 Assays of antioxidant and α-amylase inhibitory activities

### DPPH assay

DPPH radical scavenging activity was measured according to the previous report (Plaza et al., 2013). Methanol and vitamin C (Vc) were used as a blank and positive control, respectively.

### ABTS assay

The ABTS scavenging potency was assayed according to the method described by the previous report (Li et al., 2016a). Methanol and Vc were used as the blank and positive control, respectively.

### FRAP assay

The FRAP assay was carried out according to the procedure described by the previous report (Li et al., 2016b). The results were expressed as absorbance; the higher the absorbance, the stronger the reduction ability of the sample.

### Capacity to inhibit the formation of hydroxyl radical assay

The assay was performed according to the published paper (Hernández-Corroto et al., 2018). Vc was used to replace the sample as the positive control.

### α-amylase inhibitory activity

The α-amylase inhibitory activity was measured according to the method proposed by the previous report (Fu et al., 2015), and the absorbance was recorded at 540 nm.

## 2.14 Statistical analysis

All assays were performed in triplicate. The results were expressed as mean  $\pm$  SD (standard deviation). Values were expressed as mean  $\pm$  standard deviation of at least three independent experiments. The analysis of variance (ANOVA) was carried out using a significant level of 0.05. Other statistical analyses were performed using Microsoft Excel 2019. The standard curves were plotted using Origin Pro 2021 software (Version 9.8, OriginLab Corporation, Northampton, MA, USA).

## 3 Results and discussion

### 3.1 TPC and TPA analysis and calculation of PAs yield

Changes in TPC and TPA after different pretreatments are Figure 1A and Figure 1B, respectively. The TPC and TPA of the six fractions were in the order: BEP-4 > BEP-3 > BEP-1 > BEP-2 > BMP > UMP. These results showed a significant increase in TPC and TPA of PA samples after ball-milling and ball mill-assisted enzymatic hydrolysis pretreatments ( $P < 0.05$ ). In comparison with other PA samples, BEP-4 had the highest TPC ( $750.98 \pm 6.95$  mg/g extract) and TPA ( $948.72 \pm 3.50$  mg/g extract). The results showed that the combination of ball mill-assisted multi-enzymatic hydrolysis extracted more phenolic compounds and PAs than the other five methods. This may be since pretreatment with ball mill-assisted enzymatic hydrolysis can better promote the degradation of cell wall components bound to PAs, facilitating the release of more phenolics and large amounts of bound PAs (Osete-Alcaraz et al., 2019).

To further study the effect of pretreatment methods on PAs release, the yield of PAs was calculated and expressed as a percentage of the weight of PAs to each gram of the Chinese quince powder raw material. The yields of UMP, BMP, BEP-1,

BEP-2, BEP-3, and BEP-4 were 3.02%, 3.79%, 6.94%, 6.08%, 4.79%, and 7.72%, respectively. Among them, the highest yield of 7.72% could be achieved by the ball milling combined with multi-enzyme hydrolysis pretreatment method, which was 2.56 times higher than that of the conventional organic solvent extraction method. The combined use of ball milling and enzymatic hydrolysis pretreatment gave higher yields of PAs from Chinese quinces compared to ball milling pretreatment alone, and much higher yields than conventional organic solvents. Therefore, enzyme and ball milling treatments were combined to assist the extraction of PAs from Chinese quinces, as an innovative approach to replace conventional extraction methods.

### 3.2 XRD analysis

According to XRD patterns (Figure 2), the CrI of UMS was 15.8%, which was lower than all the pretreated samples. The increase in crystallinity after ball-milling was due to the removal of amorphous materials such as pectin and hemicellulose, this effect is due to the increased concentration of intact cellulose via hemicellulose and pectin solubilisation (Udeh & Erkurt, 2017). Results showed that comparing BES-1, BES-2, BES-3, and BES-4 to BMS, the CrI decreased from 22.5% to 19.6%, 16.6%, 19.7%, and 15.1%, respectively. The decrease in crystallinity after enzymatic hydrolysis pretreatment was due to the disruption of major cell wall components such as cellulose, pectin and xylan by related enzymes.

In the XRD profile of UMS, the peak at approximately  $2\theta = 22.5^\circ$  (200) indicated the cellulose had a highly ordered crystalline region. Conversely, the diffraction peak at approximately  $2\theta = 18.0^\circ$  (110) indicated a less organized amorphous region. (Phitsuwan et al., 2016). The intensity of the peak at  $2\theta = 22.5^\circ$  corresponding to the (200) lattice planes of the crystalline

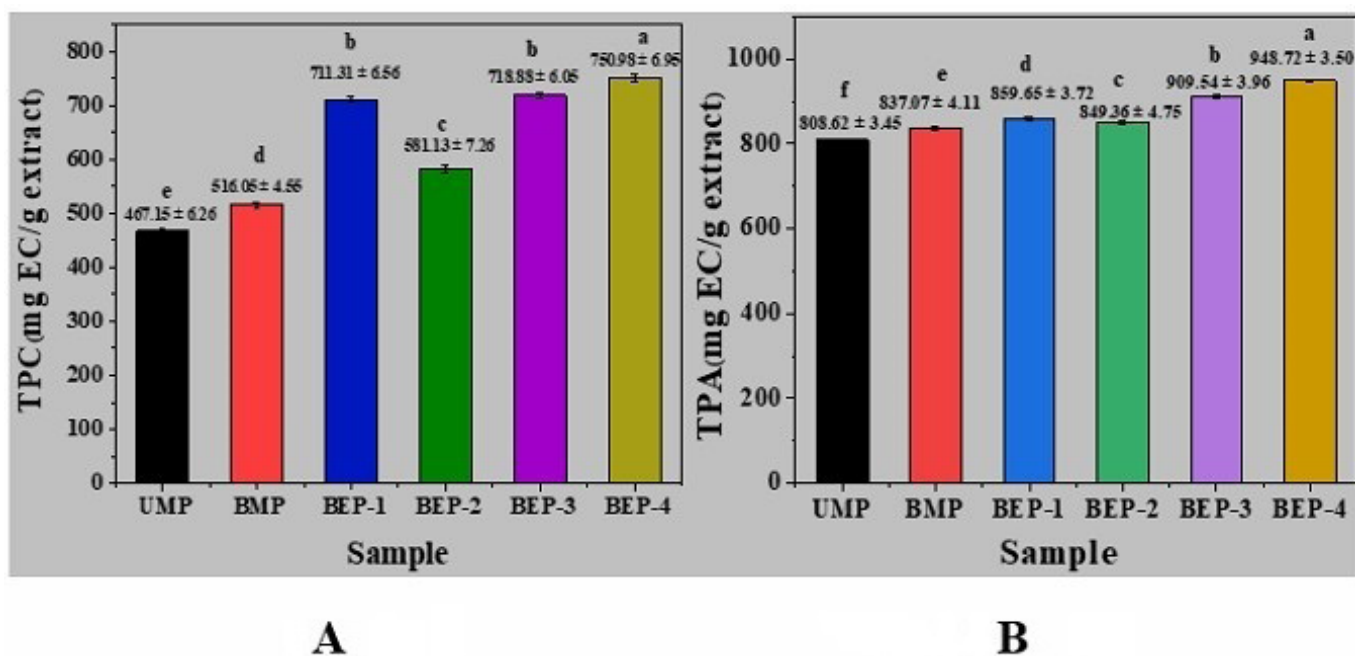


**Figure 1.** Total phenolic content (A) and total proanthocyanidin content (B) of six Chinese quince proanthocyanidins extracts. Different letters marked on different extracts are significantly different ( $P < 0.05$ ).

cellulose polymorph was increased for the samples that had been ball-milled or treated with enzymes compared to UMS, indicated that the majority of cellulose in the pretreated samples was present in crystalline state.

These findings show that a combination of enzymatic hydrolysis and ball-milling pretreatments enhances the degradation of the crystalline cellulose and other cell wall components in the cell wall of the Chinese quince.

### 3.3 SEM analysis

SEM was applied to study the surface morphology changes of Chinese quinces samples after different pretreatments and to analyze the effects of pretreatment methods on the cell wall structure. The SEM graphics of the six pretreated Chinese quince powder samples are shown in Figure 3. The results indicate that UMS had many spherical and uneven lumps, suggesting that the structures of the crystalline cellulose and other chemical components in the cell wall of the Chinese quince were not destroyed. In comparison with UMS, BMS had many smaller lumps and thick lamellas. This difference indicated that the cell wall components of the samples pretreated by ball milling had been slightly damaged. BES-1 had the thinnest sheets with irregularly folded edges and the smallest lumps in all areas, indicating that the cell wall components of the sample after enzymatic hydrolysis of cellulose were damaged the most seriously, and that the cellulolytic effect was the strongest. In comparison with UMS and BMS, BES-2, BES-3, and BES-4 had more and larger pores on the surface, as well as smaller spherical and uneven lumps, and smaller lamellar shapes. The surface of BEP-4 with the most pores and the largest pore size. Results showed that the cell walls of the samples were disrupted in varying degrees according to the different treatments; the effects of multi-enzyme and cellulose enzymatic hydrolysis were particularly remarkable. After pretreatment with enzymatic hydrolysis assisted by ball milling, the cell wall density was reduced and the cell wall surface was thin, indicating that it was damaged and became loose and

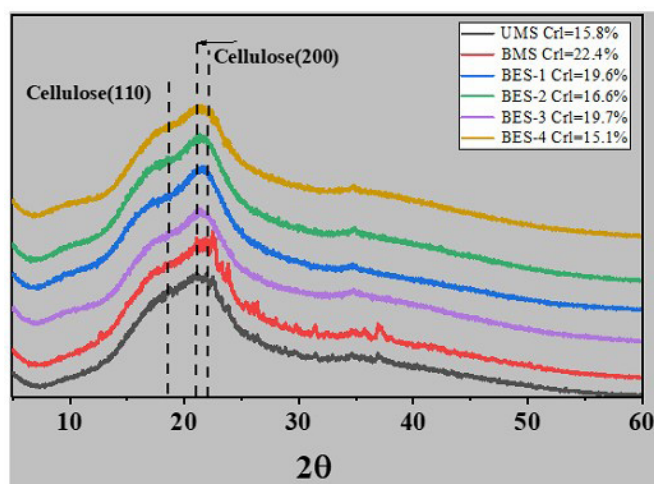


**Figure 2.** XRD patterns of untreated, ball-milled and enzymatic hydrolysed pretreated samples.

porous, which facilitated the full contact between PAs and the extraction solvent and improved the extraction efficiency.

### 3.4 FT-IR analysis

The FT-IR spectra of the six PA fractions are shown in Figure 4. All six samples exhibited an intense peak at around  $3410\text{ cm}^{-1}$ , which probably corresponds to -OH stretching in the phenolic structure of the PAs. The weaker absorption peaks at approximately  $2915\text{ cm}^{-1}$  were due to the C-H stretching vibrations assigned to the -CH and -CH<sub>2</sub> groups of the aliphatic hydrocarbons (Zhang et al., 2017). The absorption peak at  $1654\text{ cm}^{-1}$  was due to the stretching vibration of the carboxylic acid-C=O, suggesting the presence of a galloyl group on the epicatechin gallate. The most striking feature of the infrared spectrums was the dense and relatively broad band around  $1600\text{ cm}^{-1}$ . The high intensity of the C-C stretching peak at  $1606\text{ cm}^{-1}$  and  $1441\text{ cm}^{-1}$  were due to the C4-C8 interflavonoid linkages and the C-H stretching vibration of benzene rings, indicating that the core structure of the PAs was not changed significantly by ball-milling and enzymatic hydrolysis. The bands at approximately  $1380\text{ cm}^{-1}$  were due to the deformation and vibration of -C-OH, and the bands observed from  $1281\text{ cm}^{-1}$  to  $1058\text{ cm}^{-1}$  were the characteristic bands of C-O-C, including aromatic C-O and aliphatic C-O (Saive et al., 2020). The bands at  $830\text{ cm}^{-1}$  were associated with C-H of benzene rings, suggesting the presence of three hydrogens on the benzene ring. The peaks at  $764\text{ cm}^{-1}$  and  $730\text{ cm}^{-1}$  were attributed to bending vibration of -CH out-of-plane conformations of procyanidin (PC) and prodelfinidin (PD) (Fu et al., 2015). The band at  $764\text{ cm}^{-1}$  was much stronger than the band at  $730\text{ cm}^{-1}$ , indicating that Chinese quince fruit PAs contained mainly PC but a small amount of PD units (Zhang et al., 2017). The characteristic peaks of the six different PAs extracts were similar, but the signal intensities of the four BEP fractions at  $830$  and  $764\text{ cm}^{-1}$  were slightly weaker compared to the other samples, indicating partial structural damage of PAs.

### 3.5 GPC analysis

The GPC chromatograms of the six PA extracts are listed in Figure 5. Each of the six samples exhibited bimodal peaks, with the main peak at 8.5-9.5 min and a shoulder peak at 10.5-11.5 min. The six PA samples all have a low polydispersity index (PDI), which demonstrated that they were homogeneous (Jiao et al., 2020). The average  $M_w$  (weight-average molecular weight) of the six fractions were in the order: BEP-3 > BMP > BEP-2 > UMP > BEP-1 > BEP-4. The  $M_w$ ,  $M_n$  (number-average molecular weight), and PDI of BEP-1 and BEP-4 were significantly lower than the other four samples, suggesting that BEP-1 and BEP-4 may contain more low molecular weight PAs. In other words, the samples pretreated with cellulase or multiple enzymes could better release a large amount of oligomeric PAs. Meanwhile, BMP showed a higher  $M_w$  than UMP, probably because more polymeric PAs were released after ball-milling. BEP-3 has the highest  $M_w$  among the six samples. This is presumably because the pectinase pretreatment enabled solvents to infiltrate the cell wall more easily, resulting in the release of large amounts of high molar mass PA components (Yang et al., 2019b).

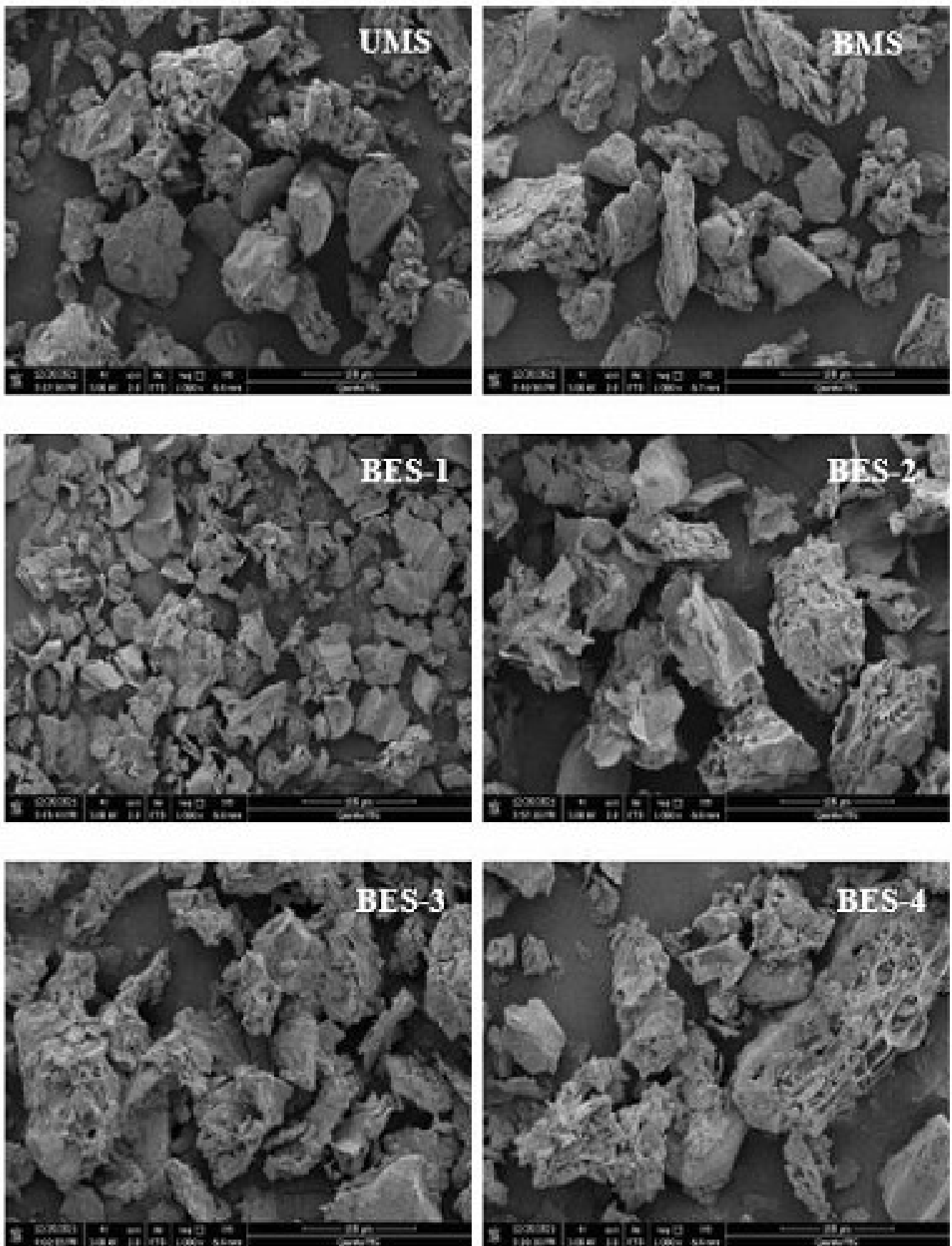


Figure 3. SEM micrographs of UMS, BMS, BES-1, BES-2, BES-3, BES-4 (1000-fold).

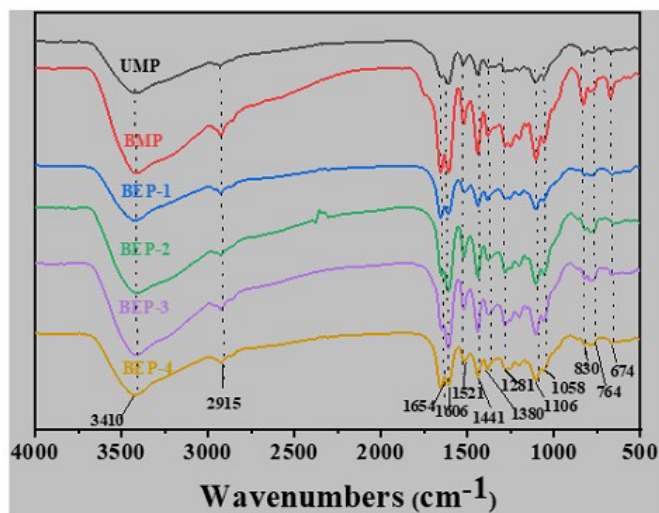


Figure 4. FT-IR spectra of UMP, BMP, BEP-1, BEP-2, BEP-3, and BEP-4.

### 3.6 Thermogravimetric analysis (TGA)

The thermal stabilities of PA extracts are closely related to the chemical composition and physical characteristics of the structural components (Phitsuwan et al., 2016). To further understand the structural differences among these PA samples, the thermal stabilities were studied by TG/DTG.

The weight loss of the six samples occurred in three stages (Figure 6A). In the first stage, ranging from 25 °C to 150 °C, there was an initial weight loss, presumably due to the loss of adsorbed water and evaporation of small molecular substances such as low molecular weight phenolic acids (Zhang et al., 2017). The second stage ranged from 150 °C to 500 °C. The rapid mass loss at this stage was associated with the breakdown of PAs (Phitsuwan et al., 2016). The third stage of weight loss was in the range of 500-700 °C, which was a carbonization process. PA decomposes depends on its structure, the substitution pattern of substituents, the degree of polymerization (DP), and

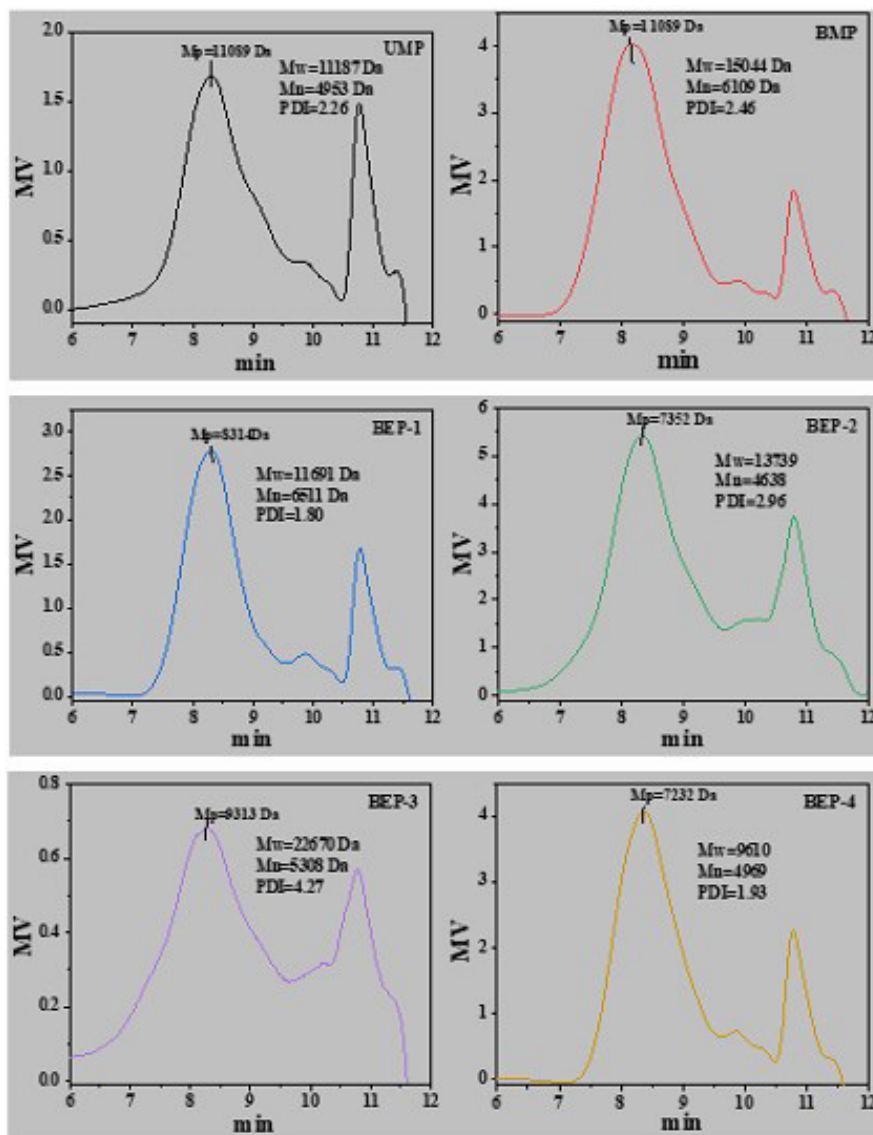
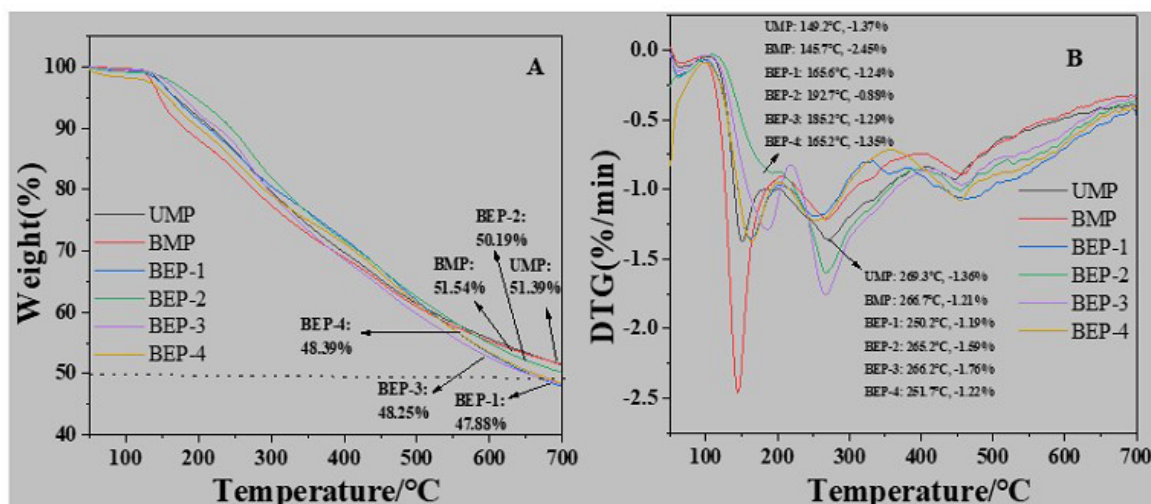


Figure 5. GPC chromatograms of various proanthocyanidin extracts isolated from the Chinese quinces by different pretreatments. MV:Electrical signals from refractive index differences.



**Figure 6.** TG curves (A) and DTG curves (B) of various proanthocyanidin extracts isolated from the Chinese quinces by different pretreatments.

the type of chemical bonds (Wen et al., 2019). As shown, UMP and BMP had higher final solid residue yields compared to the four BEP fractions. At 50% weight loss, thermal decomposition occurred at temperatures ranging from 670 °C to 680 °C for the BEP-1, BEP-3, and BEP-4 fractions, while decomposition occurred at temperatures above 700 °C for the UMP, BMP, and BEP-2 fractions. The higher the temperature at which PAs reaches 50% weight loss, the better their thermal stability. BEP-1 had the lowest temperature at 50% weight loss, indicating BEP-1 was the most unstable of the six samples. UMP and BMP had higher thermal stabilities than the four BEP fractions.

The DTG curves are shown in Figure 6B. Three notable inflection points can be seen. The inflection point occurring below 100 °C was related to the loss of water and substances such as low molecular weight phenolic acids. The second inflection point, which generally occurred at temperatures ranging from 150 °C to 200 °C, was caused by the degradation of oligomeric PAs. As can be seen from Figure 6B, during the second stage, the order of the maximum degradation temperatures was as follows: BEP-2 > BEP-3 > BEP-1 > BEP-4 > UMP > BMP, indicating that more low molecular weight PAs were isolated after pretreatment with multi-enzyme hydrolysis. The third inflection point occurred at temperatures ranging from 250 °C to 300 °C, and may be associated with the degradation of polymeric PAs (Phitsuwan et al., 2016). In the third period, the order of the maximum degradation temperatures was as follows: BMP > UMP > BEP-3 > BEP-2 > BEP-4 > BEP-1, suggesting that BMP and UMP contained more polymeric and higher molecular weight PAs than the BEP fractions. Generally, the higher the molecular weight of samples, the stronger the thermal stability. These results are consistent with those of the GPC analysis. The differences in thermal stability of PA extracts indicated differences in structure and composition among them.

### 3.7 MALDI-TOF-MS analysis

The MALDI-TOF-MS spectra of the six PAs samples are shown in Figure 7. All samples exhibited mass spectra with a primary set of peaks with differences of 288 Da (Li et al., 2016b). It can

be concluded that 288 Da is a mass difference of one catechin/epicatechin. In addition, the signal of the molecular ion peak, which was 16 Da away from the main molecular ion peak, could be detected, the signal was produced by B-type PD structures (Wang et al., 2021). These results show that the PAs in the six samples were mainly B-type PC and PD. In addition, B-type PCs were the main components of all six samples. A few molecular ion peak signals differing from the main molecular ion peak by 2 Da were also detected, indicating that A-type linkages also existed in the six samples (Chai et al., 2014). MALDI-TOF-MS analysis showed that the degree of DP of the six samples ranged from DP 3 to DP 14, with the most intensity in 4-mers, 5-mers and 6-mers. The DP distribution of oligomers in the UMP and BMP fractions were mainly concentrated in DP3 and DP4, the DP distribution of oligomers in the BEP-1 and BEP-4 fractions were mainly concentrated in DP7, DP8, and DP9, and the DP distribution of oligomers in the BEP-2 and BEP-3 fractions were mainly concentrated in DP5 and DP6.

### 3.8 LC-MS/MS analysis

The main constituents of oligomeric PAs of six PA extracts were analyzed by LC-MS/MS, and the results are shown in Table 1. A total of nine PA oligomers were detected. There were five flavan-3-ol basic units, namely, catechin, epicatechin, epicatechin gallate, and epigallocatechin-3-gallate, PA dimer (PB2), PA trimer (PC1), and PA tetramer. The highest content of PA trimer was found among these oligomers. This result was consistent with our previous study (Wang et al., 2021).

As shown in Table 1, the order of oligomer content was BMP > UMP > BEP-3 > BEP-2 > BEP-4 > BEP-1. UMP, BMP, and BEP-1 contained relatively high proportions of catechins and epicatechins—namely, 22.32%, 65.22%, and 18.46%, respectively. Epigallocatechin gallate (7.51%) in BEP-1 was higher than in the other five fractions. Epigallocatechin-3-gallate (7.44%) in BEP-3 was higher than in the other five fractions. PC1 in BEP-4 was higher than in the other fractions, up to 73.49% of oligomers. PA tetramers in BEP-2 and BEP-3 were higher, up to 5.11% and 5.38%, respectively. As shown in Table 1, the

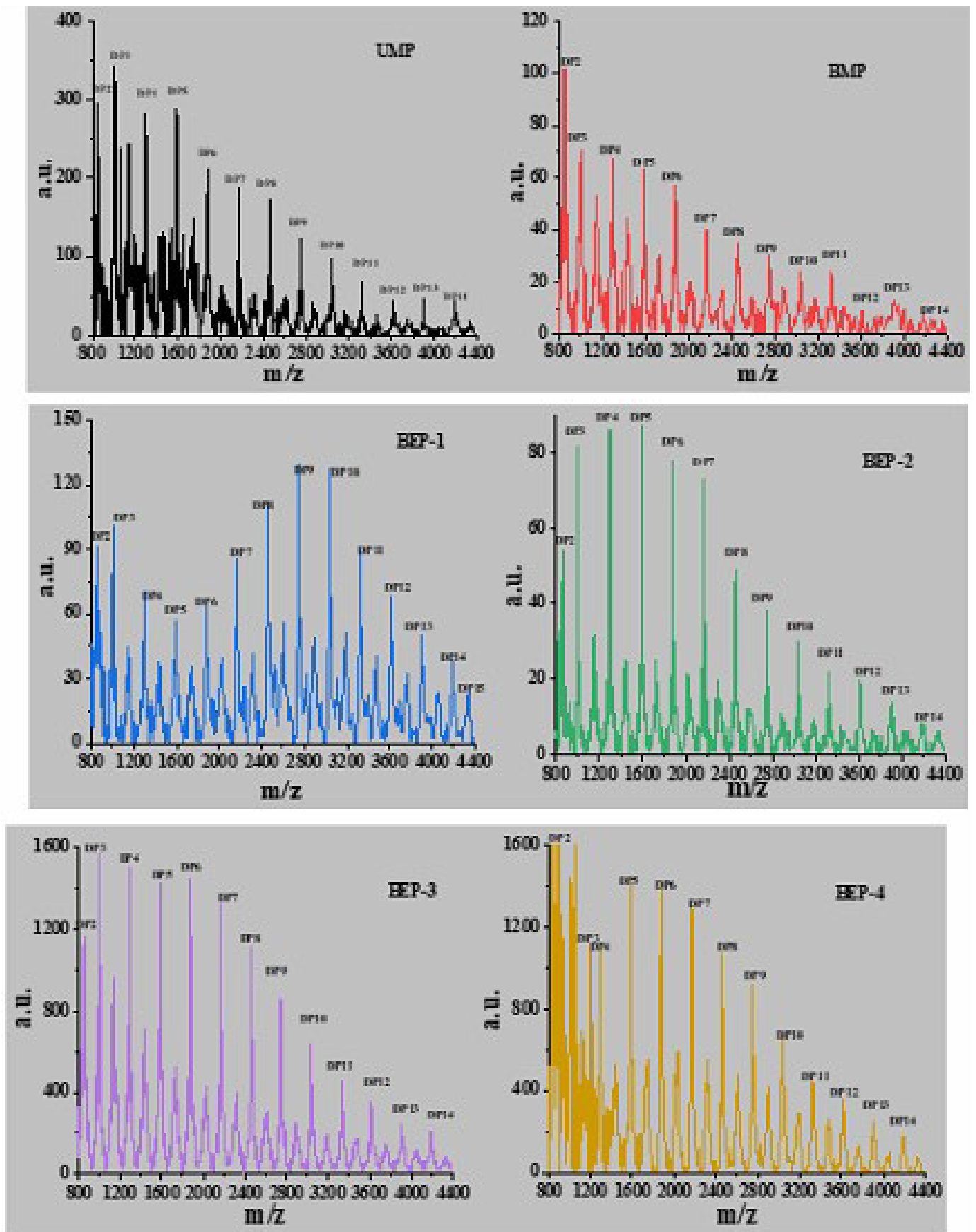


Figure 7. MALDI-TOF-MS spectra of various proanthocyanidin extracts isolated from Chinese quinces by different pretreatments.

**Table 1.** The content of compounds (ug/mg extracts) in various proanthocyanidins extracts and percentage content (%) of each component based on total oligomeric procyanidins.

	UMP		BMP		BEP-1		BEP-2		BEP-3		BEP-4	
	ug/mg	%										
<b>Catechin/epicatechin</b>	2.64	22.32	9.34	65.22	0.60	18.46	0.70	8.82	0.80	9.91	0.54	11.64
<b>epicatechin gallate</b>	0.27	2.29	0.11	0.78	0.24	7.51	0.19	2.45	0.11	1.32	0.13	2.82
<b>Epigallocatechin-3-gallate</b>	0.11	0.89	0.11	0.79	0.17	5.30	0.09	1.10	0.60	7.44	0.09	1.95
<b>Procyanidin B2</b>	1.34	11.33	1.04	7.26	0.22	6.77	0.88	11.08	1.26	15.61	0.24	5.17
<b>procyanidin C1</b>	7.0	59.17	3.34	23.32	1.88	57.85	5.66	71.28	4.86	60.22	3.41	73.49
<b>Procyanidin tetramer</b>	0.46	3.91	0.37	2.60	0.13	4.08	0.41	5.11	0.43	5.38	0.22	4.80
<b>Oligomeric procyanidins</b>	11.83	-	14.32	-	3.25	-	7.94	-	8.07	-	4.64	-

content of oligomers in the BEP fraction was slightly reduced compared to the UMP and BMP fractions, which may be due to the fact that PA oligomers had more hydroxyl groups in their molecules and are less stable, and loss of some oligomers during the enzymatic pretreatment.

### 3.9 2D-HSQC NMR analysis

The 2D-HSQC NMR spectra are displayed in Figure 8. The attribution of signals is based on previous publications (Saive et al., 2020; Reeves et al., 2020; Crestini et al., 2016). We selected the most representative BEP-4 from the four samples treated by enzymatic hydrolysis and performed NMR analysis on them, together with UMP and BMP. In the NMR spectra, UMP, BMP, and BEP-4 showed strong and similar signals, with only slight differences, indicating that the different pretreatments had not significantly changed the “core” of the PC structure. More specifically, the signals at  $\delta C/\delta H$  112-120/6.4-7.4 ppm were present in the spectra of UMP, BMP, and BEP-4 HSQC, which correspond to the C2'-H2', C5'-H5', C6'-H6' correlations peak for B-ring substitution pattern of PC structures. The signals at  $\delta C/\delta H$  92-96/5.8-6.2 ppm appeared in both UMP and BEP-4 HSQC spectra, but not in the HSQC spectrum of BMP, which correspond to the C6-H6, C8-H8 correlations peaks for phloroglucinol units of PD structures. The C2-H2 (trans/cis) correlation peaks for A-ring substitution pattern, C4-H4 correlation peaks for A-ring substitution pattern, C4-H4 (trans/cis) correlations for B-ring substitution pattern, and non-aromatic hydroxylated C-H occurring at  $\delta C/\delta H$  74-78/4.8-5.6 ppm,  $\delta C/\delta H$  26-29/2.7-3.0 ppm,  $\delta C/\delta H$  36-38/4.2-4.8 ppm, and  $\delta C/\delta H$  68-72/3.4-4.2 ppm, respectively, were present in all UMP, BMP, and BEP-4 HSQC spectra.

The HSQC analysis confirmed the presence of PC and PD structures in the PA samples and provided information about the composition and structural subtypes. HSQC results suggest that the PAs in the three samples were mainly cis-conformation PC structures. In addition, the difference in peak areas of the signal peaks of different extracts showed that the BEP-4 contained a higher proportion of PC structure (98.35%) and flavan-3-ol content (87.88%) compared to UMP and BMP.

### 3.10 Antioxidant capacity and biological activity analysis

#### Antioxidant capacity

DPPH, ABTS, FRAP, and OH radical scavenging in vitro assays were used to evaluate the antioxidant capacity of six PA extracts. As shown in Figure 9, the scavenging abilities of all samples increased with increasing concentration and reached maximum values. Among them, the scavenging activity of BEP-4 was the highest, nearly 100%. The results of DPPH, ABTS, OH and FRAP assays showed consistent trends. The radical scavenging activity could also be indicated as the antioxidant concentration required for a 50% radical reduction ( $IC_{50}$ ) (Li et al., 2016; Lv et al., 2015). The  $IC_{50}$  values of these samples are shown in Table 2. BEP-4, with the highest PA content, showed the lowest  $IC_{50}$  values and the highest antioxidant capacity. Obviously, the radical scavenging activities of BEP-1, BEP-2, BEP-3, and BMP are higher than that of UMP, but lower than BEP-4 ( $P < 0.05$ ). All six samples showed higher radical scavenging capacities than Vc ( $P < 0.05$ ).

Overall, the ferric ion reducing ability of PA samples pretreated by ball milling and ball milling assisted enzymatic hydrolysis was higher than that of the untreated sample. Antioxidants scavenge free radicals by providing electrons through the action of their reducing power. Therefore, the strength of reducing ability reflects the strength of antioxidant free radical scavenging ability (Erdogan-Orhan et al., 2019). The results of reducing ability were similar to ABTS, OH, and DPPH assays. Thus, in a reducing agent-like manner, phenolic compounds provide electrons and react with free radicals, converting them into more stable products, terminating the chain reaction of free radicals, and inhibiting oxidation (Li et al., 2015b).

The PA and phenol content of samples determine their antioxidant ability (Jiang et al., 2016; Aladedunye et al., 2014). In general, phenolic hydroxyl groups have a positive effect on the antioxidant activity of PA samples, and the higher TPC and TPA, the more phenolic hydroxyl groups they have, the stronger their antioxidant activity along with (Osete-Alcaraz et al., 2019; Shang et al., 2022). In addition, there was a correlation between antioxidant activity and its molecular weight in addition to the phenolic hydroxyl content. A previous report (Dorenkott et al.,

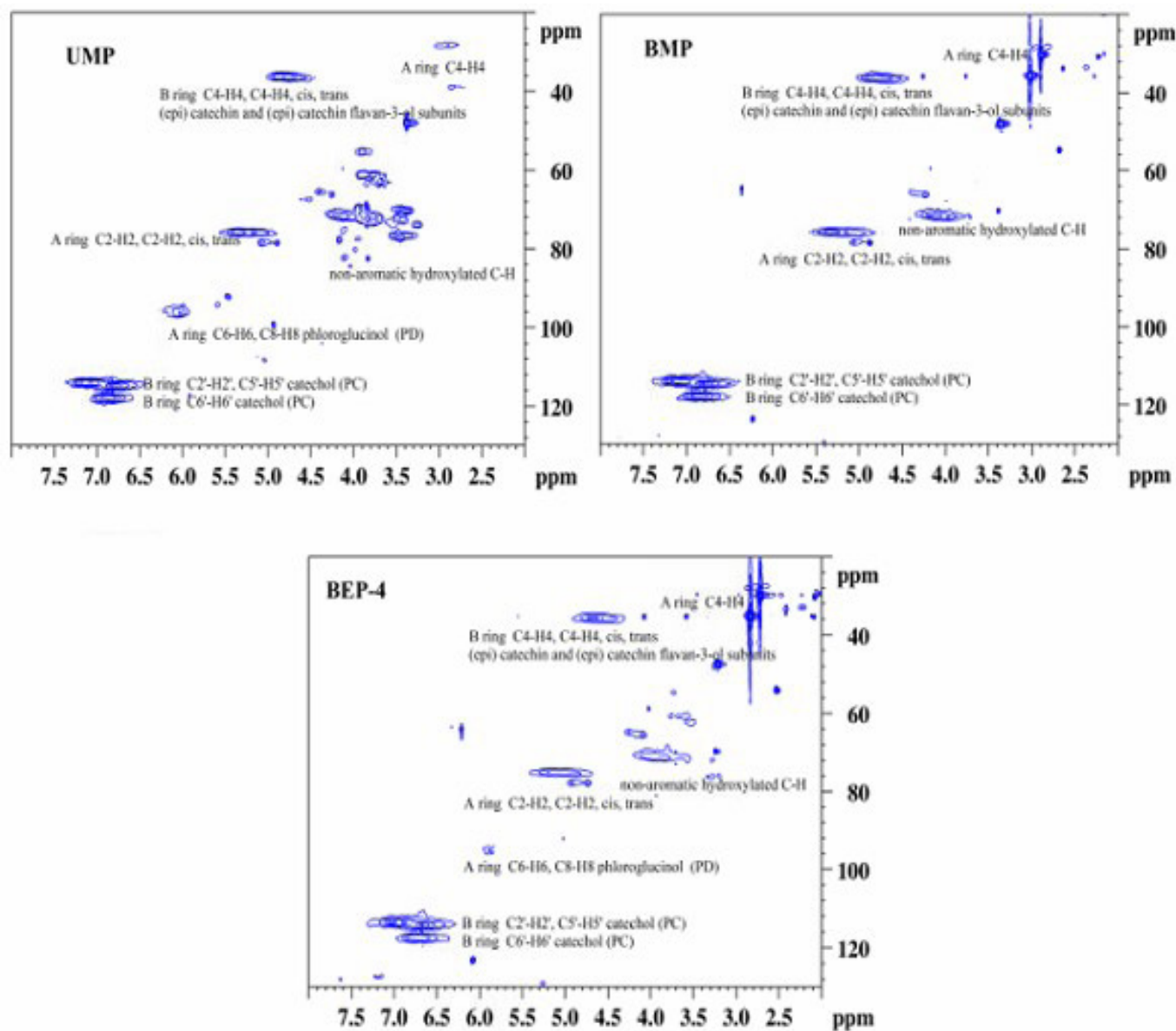


**Figure 8.** HSQC NMR spectrum of three proanthocyanidin samples isolated from Chinese quinces after different pretreatments.

2014) has shown that PAs with lower DP and  $M_w$  have the stronger antioxidant capacity and biological activities. The molecular weight results showed that BEP-4 had the lowest molecular weight and the strongest antioxidant activity. Wang et al. (2012) report confirmed that PAs have more free radical scavenging activity at lower molecular weights. The results of DPPH, ABTS, OH and FRAP assays for six samples were consistent with their molecular weight results. The antioxidant activity of PAs may be also influenced by their chemical structures, including monomeric units, DP, PDI and linkage types. For example, compared with other PA fractions, BEP-1 and BEP-4 fractions have lower PDI and exhibit higher antioxidant activity.

#### *$\alpha$ -amylase inhibitory capacity*

$\alpha$ -Amylase is an endo-acting enzyme that is a key enzyme in the digestion of carbohydrates in the human diet.  $\alpha$ -Amylase

inhibitors slow carbohydrate digestion and delay glucose absorption, thereby slowing postprandial blood glucose elevation. In recent years, natural and novel  $\alpha$ -amylase inhibitors are mostly derived from plant sources such as phenolic compounds. Since the PA extracts possess a large number of phenolic compounds and PAs, they may have many potential interaction sites and therefore may bind to several protein molecules, thus acting as an inhibitor of  $\alpha$ -amylase activity. The inhibitory activities of six PA extracts against  $\alpha$ -amylase were investigated.

As shown in Figure 9E, UMP, BMP, BEP-1, BEP-2, BEP-3, and BEP-4 showed inhibitions up to 77.00%, 81.66%, 84.14%, 83.59%, 86.82%, and 92.98%, respectively.  $IC_{50}$  values of six samples are shown in Table 2. BEP-4 showed the highest inhibitory effect with the lowest  $IC_{50}$  value ( $P < 0.05$ ) (Sun et al., 2016). Fu et al. (2015) also demonstrated that PAs from longan was effective in inhibiting  $\alpha$ -amylase activity. This is due to the interaction

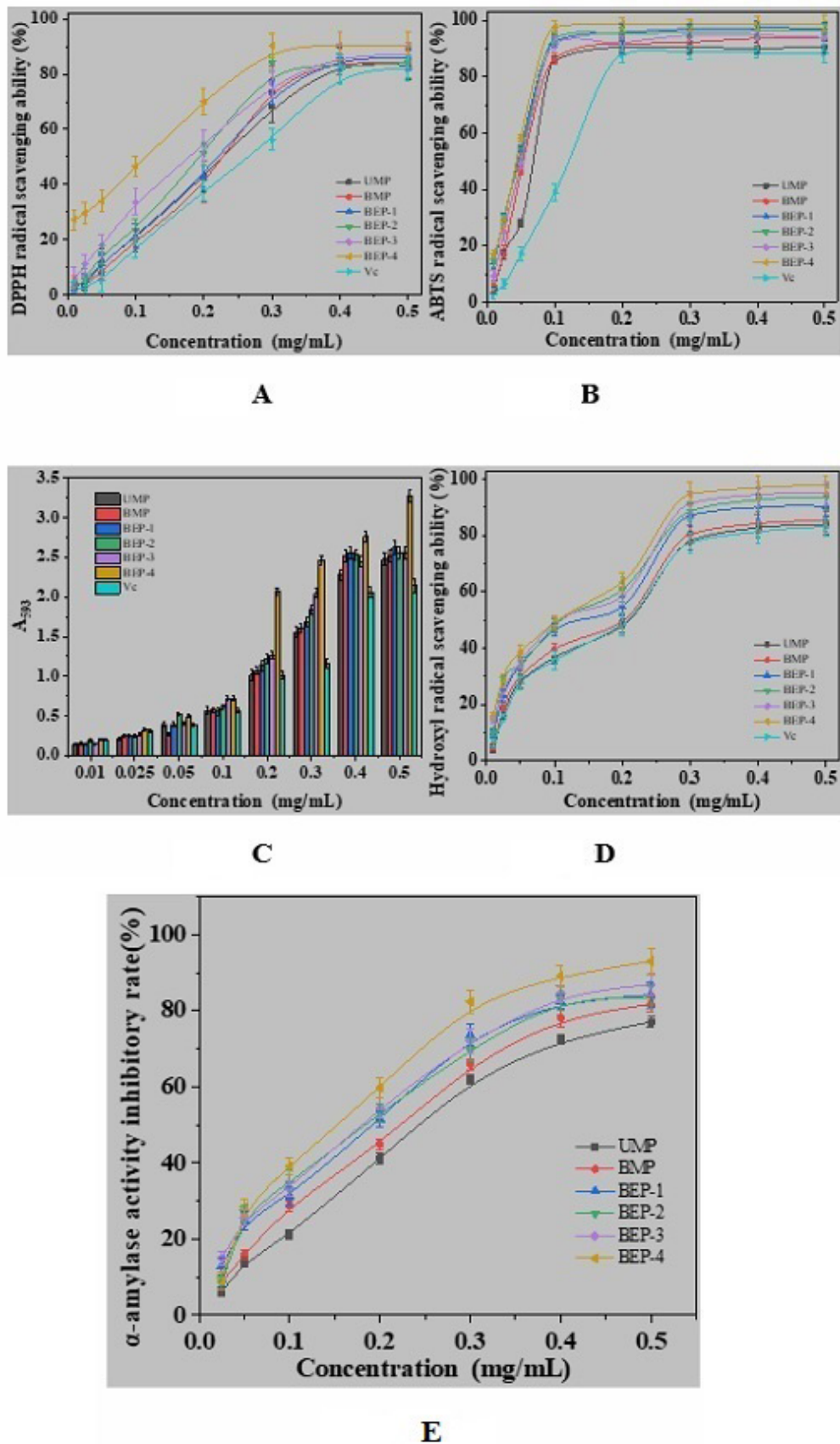


**Figure 9.** Antioxidant activity against DPPH (A), ABTS (B), ferric ion reducing antioxidant power (C), hydroxyl radical formation inhibition capacity (D),  $\alpha$ -Amylase inhibitory capacity (E) of UMP, BMP, BEP-1, BEP-2, BEP-3, BEP-4, and Vc.

**Table 2.** Free radical-scavenging activity (IC<sub>50</sub>) of six proanthocyanidins extracts isolated from Chinese quince fruits.

Sample	DPPH	ABTS	OH	α-amylase
	IC <sub>50</sub> (μg/mL)	IC <sub>50</sub> (μg/mL)	IC <sub>50</sub> (μg/mL)	IC <sub>50</sub> (μg/mL)
UMP	253.87 ± 5.06 <sup>b</sup>	122.67 ± 1.47 <sup>b</sup>	215.47 ± 0.51 <sup>b</sup>	276.58 ± 0.52 <sup>a</sup>
BMP	250.57 ± 4.88 <sup>b</sup>	94.55 ± 0.54 <sup>c</sup>	203.75 ± 1.57 <sup>c</sup>	248.20 ± 0.76 <sup>b</sup>
BEP-1	244.80 ± 1.82 <sup>c</sup>	42.15 ± 0.68 <sup>e</sup>	170.56 ± 0.66 <sup>d</sup>	215.23 ± 0.67 <sup>c</sup>
BEP-2	232.57 ± 1.44 <sup>d</sup>	41.91 ± 0.45 <sup>e</sup>	156.25 ± 0.77 <sup>e</sup>	215.97 ± 0.88 <sup>c</sup>
BEP-3	216.71 ± 0.89 <sup>e</sup>	68.64 ± 0.56 <sup>d</sup>	151.18 ± 0.39 <sup>f</sup>	205.36 ± 0.31 <sup>d</sup>
BEP-4	131.45 ± 0.97 <sup>f</sup>	22.66 ± 0.32 <sup>f</sup>	134.05 ± 0.71 <sup>g</sup>	182.07 ± 0.28 <sup>e</sup>
Vc	276.23 ± 1.31 <sup>a</sup>	185.45 ± 0.26 <sup>a</sup>	217.54 ± 0.90 <sup>a</sup>	--

Values are expressed as mean ± standard deviation (n=3). Different superscript letters in every column represent significantly different mean values (p<0.05).

of PAs with α-amylase, which impedes the enzyme activity by covalently binding α-amylase (Iftikhar et al., 2020). Compared with the conventional method, the extracts after ball milling-assisted enzymatic hydrolysis pretreatment had higher TPC and TPA, and thus they had more potential interaction sites for better inhibition of amylase activity (Quan et al., 2019). Thus, the results of these experiments indicate that enzyme hydrolysis and ball-milling as pretreatments of Chinese quince fruits improve the α-amylase inhibitory ability of extracted PAs.

#### 4 Conclusion

In the present investigation, ball milling and enzymatic hydrolysis were used as pretreatments for Chinese quince fruits before PA extraction by organic solvent. The sample treated with ball-milling and multi-enzyme (cellulase, xylanase, and pectinase) hydrolysis (BEP-4) extraction yield was 77.23 ± 0.71 mg/g of dry weight Chinese quince powder, which was much higher than that of conventional organic solvents (30.15 ± 0.56 mg/g). The BEP-4 also had the highest total phenolic and PA contents, namely 750.98 ± 6.95 and 948.72 ± 3.50 mg/g of dry weight extract, respectively. However, the thermal stability, PDI (1.93) and  $M_w$  (9610 Da) of BEP-4 were lower than other fractions. The combination of enzymatic hydrolysis and ball-milling pretreatments enhanced the destruction of chemical components in the cell walls. The six PA samples were structurally similar, mainly consisting of B-type PC structures, and the core structure of PA extracts did not change after different pretreatment methods, maintaining the structural integrity. BEP-4 had a high percentage of PC structure (98.35%) and flavan-3-ol content (87.88%). BEP-4 also had the highest antioxidant activity among all the samples. It had the highest antioxidant capacity with IC<sub>50</sub> values of 131.45 ± 0.97, 22.66 ± 0.32, 134.05 ± 0.71, and 182.07 ± 0.28 μg/mL for DPPH, ABTS, hydroxyl radical scavenging capacity, and α-amylase inhibiting capacity, respectively. Overall, the combination of ball-milling and enzyme assistance improved the extraction of PAs from Chinese quince fruits, giving higher yields with higher purity and greater antioxidant activity. The results of this investigation provided experimental support for developing Chinese quince fruit PAs as natural antioxidants.

#### References

Aladedunye, F., Przybylski, R., Niehaus, K., Bednarz, H., & Matthaues, B. (2014). Phenolic extracts from *Crataegus × mordenensis* and *prunus virginiana*: composition, antioxidant activity and performance in

sunflower oil. *Lebensmittel-Wissenschaft + Technologie*, 59(1), 308-319. <http://dx.doi.org/10.1016/j.lwt.2014.06.002>.

- Cascaes-Teles, A. S., Hidalgo-Chavez, D. W., Zarur-Coelho, M. A., Rosenthal, A., Fortes-Gottschalk, L. M., & Tonon, R. V. (2021). Combination of enzyme-assisted extraction and high hydrostatic pressure for phenolic compounds recovery from grape pomace. *Journal of Food Engineering*, 288, 110-128. <http://dx.doi.org/10.1016/j.foodeng.2020.110128>.
- Chai, W. M., Chen, C. M., Gao, Y. S., Feng, H. L., Ding, Y. M., Shi, Y., Zhou, H. T., & Chen, Q. X. (2014). Structural analysis of proanthocyanidins isolated from fruit stone of Chinese hawthorn with potent antityrosinase and antioxidant activity. *Journal of Agricultural and Food Chemistry*, 62(1), 123-129. <http://dx.doi.org/10.1021/jf405385j>. PMID:24313351.
- Crestini, C., Lange, H., & Bianchetti, G. (2016). Detailed chemical composition of condensed tannins via quantitative <sup>31</sup>P NMR and HSQC analyses: acacia catechu, schinopsis balansae, and acacia mearnsii. *Journal of Natural Products*, 79(9), 2287-2295. <http://dx.doi.org/10.1021/acs.jnatprod.6b00380>. PMID:27551744.
- Domínguez-Rodríguez, G., Marina, M. L., & Plaza, M. (2017). Strategies for the extraction and analysis of non-extractable polyphenols from plants. *Journal of Chromatography. A*, 1514, 1-15. <http://dx.doi.org/10.1016/j.chroma.2017.07.066>. PMID:28778531.
- Dorenkott, M., Griffin, L., Goodrich, K., Thompson-Witrick, K., Fundaro, G., Ye, L., Stevens, J., Ali, M., O'Keefe, S., Hulver, M., & Neilson, A. (2014). Oligomeric cocoa procyanidins possess enhanced bioactivity compared to monomeric and polymeric cocoa procyanidins for preventing the development of obesity, insulin resistance, and impaired glucose tolerance during high-fat feeding. *Journal of Agricultural and Food Chemistry*, 62(10), 2216-2227. <http://dx.doi.org/10.1021/jf500333y>. PMID:24559282.
- Erdogan-Orhan, I., Küpeli-Akkol, E., Sutar, I., & Yesilada, E. (2019). Assessment of anticholinesterase and antioxidant properties of the extracts and (+)-catechin obtained from *arceuthobium oxycedri* (D.C.) M. Bieb. (*dwarf mistletoe*). *South African Journal of Botany*, 120, 309-312. <http://dx.doi.org/10.1016/j.sajb.2018.09.023>.
- Esquivel-Alvarado, D., Alfaro-Viquez, E., Krueger, C. G., Vestling, M. M., & Reed, J. D. (2021). Classification of proanthocyanidin profiles using matrix-assisted laser desorption/ionization time-of-flight mass spectrometry (MALDI-TOF-MS) spectra data combined with multivariate analysis. *Food Chemistry*, 336, 127667. <http://dx.doi.org/10.1016/j.foodchem.2020.127667>. PMID:32758802.
- Fernandes, P. A., Le Bourvellec, C., Renard, C., Wessel, D. F., Cardoso, S. M., & Coimbra, M. A. (2020). Interactions of arabinan-rich pectic polysaccharides with polyphenols. *Carbohydrate Polymers*, 230, 115644. <http://dx.doi.org/10.1016/j.carbpol.2019.115644>. PMID:31887907.

- Fraser, K., Collette, V., & Hancock, K. R. (2016). Characterisation of proanthocyanidins from seeds of perennial ryegrass (*Lolium perenne* L.) and tall fescue (*Festuca arundinacea*) by liquid chromatography/mass spectrometry. *Journal of Agricultural and Food Chemistry*, 64(35), 6676-6684. <http://dx.doi.org/10.1021/acs.jafc.6b02563>.
- Fu, C., Yang, X., Lai, S., Liu, C., Huang, S., & Yang, H. (2015). Structure, antioxidant and  $\alpha$ -amylase inhibitory activities of longan proanthocyanidins. *Journal of Functional Foods*, 14, 23-32. <http://dx.doi.org/10.1016/j.jff.2015.01.041>.
- Hamauzu, Y., & Mizuno, Y. (2014). Extractable and non-extractable procyanidins enhance a food function of dietary fiber in Chinese quince and quince fruits. *Acta Horticulturae*, (1040), 125-132. <http://dx.doi.org/10.17660/ActaHortic.2014.1040.16>.
- Hernández-Corroto, E., Marina, M. L., & García, M. C. (2018). Multiple protective effect of peptides released from olea europaea and prunus persica seeds against oxidative damage and cancer cell proliferation. *Food Research International*, 106, 458-467. <http://dx.doi.org/10.1016/j.foodres.2018.01.015>. PMID:29579948.
- Huang, C., He, J., Li, X., Min, D., & Yong, Q. (2015). Facilitating the enzymatic saccharification of pulped bamboo residues by degrading the remained xylan and lignin-carbohydrates complexes. *Bioresource Technology*, 192, 471-477. <http://dx.doi.org/10.1016/j.biortech.2015.06.008>. PMID:26080104.
- Iftikhar, M., Zhang, H. J., Iftikhar, A., Raza, A., Begum, N., Tahamina, A., Syed, H., Khan, M., & Wang, J. (2020). Study on optimization of ultrasonic assisted extraction of phenolic compounds from rye bran. *Lebensmittel-Wissenschaft + Technologie*, 134, 110243. <http://dx.doi.org/10.1016/j.lwt.2020.110243>.
- Jiang, G. Q., Zhang, Z. R., Li, L. L., Du, F. G., & Pang, J. Y. (2016). Analysis of purified oligomeric proanthocyanidins from *Larix gmelinii* bark and the study of physiological activity of the purified product. *BioResources*, 11(1), 1690-1706. <http://dx.doi.org/10.15376/biores.11.1.1690-1706>.
- Jiao, S. L., Li, Y., Wang, Z. S., Sun-Waterhouse, D. X., Waterhouse, G. I. N., Liu, C. F., & Wang, X. L. (2020). Optimization of enzyme-assisted extraction of bioactive-rich juice from *Chaenomeles sinensis* (Thouin) Koehne by response surface methodology. *Journal of Food Processing and Preservation*, 44(9), e14638. <http://dx.doi.org/10.1111/jfpp.14638>.
- Li, Q., Chen, J., Li, T., Liu, C. M., Wang, X. Y., Dai, T. T., McClements, D. J., & Liu, J. Y. (2015a). Impact of in vitro simulated digestion on the potential health benefits of proanthocyanidins from *Choerospondias axillaris* peels. *Food Research International*, 78, 378-387. <http://dx.doi.org/10.1016/j.foodres.2015.09.004>. PMID:28433306.
- Li, Z., Zeng, J., Tong, Z., Qi, Y., & Gu, L. (2015b). Hydrogenolytic depolymerization of procyanidin polymers from hi-tannin Sorghum Bran. *Food Chemistry*, 188, 337-342. <http://dx.doi.org/10.1016/j.foodchem.2015.05.021>. PMID:26041201.
- Li, Q., Chen, J., Li, T., Liu, C., Liu, W., & Liu, J. (2016a). Comparison of bioactivities and phenolic composition of *choerospondias axillaris* peels and flesh. *Journal of the Science of Food and Agriculture*, 96(7), 2462-2471. <http://dx.doi.org/10.1002/jsfa.7366>. PMID:26249806.
- Li, Q., Wang, X. L., Chen, J., Liu, C. M., Li, T., McClements, D. J., Dai, T. T., & Liu, J. Y. (2016b). Antioxidant activity of proanthocyanidins-rich fractions from *choerospondias axillaris* peels using a combination of chemical-based methods and cellular-based assay. *Food Chemistry*, 208, 309-317. <http://dx.doi.org/10.1016/j.foodchem.2016.04.012>. PMID:27132855.
- Li, X., Liu, J., Chang, Q., Zhou, Z. Y., Han, R. L., & Liang, Z. S. (2021). Antioxidant and antidiabetic activity of proanthocyanidins from *Fagopyrum dibotrys*. *Molecules*, 26(9), 2417-2439. <http://dx.doi.org/10.3390/molecules26092417>. PMID:33919259.
- Liu, B., Wang, H., Hu, T., Zhang, P., Zhang, Z., Pan, S., & Hu, H. (2017). Ball-milling changed the physicochemical properties of SPI and its cold-set gels. *Journal of Food Engineering*, 195, 158-165. <http://dx.doi.org/10.1016/j.jfoodeng.2016.10.006>.
- Lv, Q., Luo, F., Zhao, X., Liu, Y., Hu, G., Sun, C., Li, X., & Chen, K. (2015). Identification of proanthocyanidins from *Litchi* (*Litchi chinensis* Sonn.) pulp by LC-ESI-Q-TOF-MS and their antioxidant activity. *PLoS One*, 10(3), e0120480. <http://dx.doi.org/10.1371/journal.pone.0120480>. PMID:25793378.
- Lv, T. T., Qin, Z., Wang, S. T., Liu, H. M., Ma, Y. X., Zheng, Y. Z., & Wang, X. D. (2021). Effect of proanthocyanidin-rich extracts from Chinese quince (*Chaenomeles sinensis*) fruit on the physical and oxidative stability of sunflower oil-in-water emulsions. *International Journal of Food Science & Technology*, 56(11), 5547-5559. <http://dx.doi.org/10.1111/ijfs.15114>.
- Osete-Alcaraz, A., Bautista-Ortín, A. B., Ortega-Regules, A. E., & Gómez-Plaza, E. (2019). Combined use of pectolytic enzymes and ultrasounds for improving the extraction of phenolic compounds during vinification. *Food and Bioprocess Technology*, 12(8), 1330-1339. <http://dx.doi.org/10.1007/s11947-019-02303-0>.
- Phitsuwan, P., Sakka, K., & Ratanakhanokchai, K. (2016). Structural changes and enzymatic response of Napier grass (*Pennisetum purpureum*) stem induced by alkaline pretreatment. *Bioresource Technology*, 218, 247-256. <http://dx.doi.org/10.1016/j.biortech.2016.06.089>. PMID:27371797.
- Plaza, M., Abrahamsson, V., & Turner, C. (2013). Extraction and neoformation of antioxidant compounds by pressurized hot water extraction from apple byproducts. *Journal of Agricultural and Food Chemistry*, 61(23), 5500-5510. <http://dx.doi.org/10.1021/jf400584f>. PMID:23675866.
- Qi, Y., Zhang, H., Awika, J. M., Wang, L., Qian, H., & Gu, L. (2016). Depolymerization of sorghum procyanidin polymers into oligomers using HCl and epicatechin: reaction kinetics and optimization. *Journal of Cereal Science*, 70, 170-176. <http://dx.doi.org/10.1016/j.jcs.2016.06.002>.
- Qin, Z., Liu, H. M., Lv, T. T., & Wang, X. D. (2020). Structure, rheological, thermal and antioxidant properties of cell wall polysaccharides from Chinese quince fruits. *International Journal of Biological Macromolecules*, 147, 1146-1155. <http://dx.doi.org/10.1016/j.ijbiomac.2019.10.083>. PMID:31726165.
- Qin, Z., Wang, X. D., Liu, H. M., Wang, D. M., & Qin, G. Y. (2018). Structural characterization of Chinese quince fruit lignin pretreated with enzymatic hydrolysis. *Bioresource Technology*, 262, 212-220. <http://dx.doi.org/10.1016/j.biortech.2018.04.072>. PMID:29709839.
- Quan, N. V., Xuan, T. D., Tran, H. D., Thuy, N. T. D., Trang, L. T., Huong, C. T., Andriana, Y., & Tuyen, P. T. (2019). Antioxidant,  $\alpha$ -amylase and  $\alpha$ -glucosidase inhibitory activities and potential constituents of *Canarium tramdenum* bark. *Molecules*, 24(3), 605-619. <http://dx.doi.org/10.3390/molecules24030605>. PMID:30744084.
- Reeves, S. G., Somogyi, A., Zeller, W. E., Ramelot, T. A., Wrighton, K. C., & Hagerman, A. E. (2020). Proanthocyanidin structural details revealed by ultrahigh resolution FT-ICR MALDI-mass spectrometry,  $^1\text{H}$ - $^{13}\text{C}$  HSQC NMR, and thiolysis-HPLC-DAD. *Journal of Agricultural and Food Chemistry*, 68(47), 14038-14048. <http://dx.doi.org/10.1021/acs.jafc.0c04877>. PMID:33170695.
- Roy, R., Jadhav, B., Rahman, M. S., & Raynie, D. E. (2021). Characterization of residue from catalytic hydrothermal depolymerization of lignin. *Current Research in Green and Sustainable Chemistry*, 4, 100052. <http://dx.doi.org/10.1016/j.crgsc.2020.100052>.
- Saive, M., Genva, M., Istasse, T., Frederich, M., Maes, C., & Fauconnier, M. L. (2020). Identification of a proanthocyanidin from *Litchi chinensis* Sonn. root with anti-tyrosinase and antioxidant activity.

- Biomolecules*, 10(9), 1347-1362. <http://dx.doi.org/10.3390/biom10091347>. PMID:32967274.
- Sawai-Kuroda, R., Kikuchi, S., Shimizu, K. Y., Sasaki, Y., Kuroda, K., Tanaka, T., Yamamoto, T., Sakurai, K., & Shimizu, K. (2013). A polyphenol-rich extract from *Chaenomeles Sinensis* (Chinese quince) inhibits influenza A virus infection by preventing primary transcription in vitro. *Journal of Ethnopharmacology*, 146(3), 866-872. <http://dx.doi.org/10.1016/j.jep.2013.02.020>. PMID:23439031.
- Shahidi, F., & Yeo, J. D. (2016). Insoluble-bound phenolics in food. *Molecules*, 21(9), 1216-1238. <http://dx.doi.org/10.3390/molecules21091216>. PMID:27626402.
- Shang, Y. F., Zhang, T. H., Thakur, K., Zhang, G. H., Cespedes-Acuna, C. L. A., & Wei, Z. H. (2022). HPLC-MS/MS targeting analysis of phenolics metabolism and antioxidant activity of extractions from *Lycium barbarum* and its meal using different methods. *Food Science and Technology*, 42, e71022. <http://dx.doi.org/10.1590/fst.71022>.
- Silva, T., Nogueira, J., Rezende, Y., Oliveira, C., & Narain, N. (2022). Bioactive compounds and antioxidants activities in the agro-industrial residues of berries by solvent and enzyme assisted extraction. *Food Science and Technology*, 42, e61022. <http://dx.doi.org/10.1590/fst.61022>.
- Sun, L. J., Warren, F. J., Netzel, G., & Gidley, M. J. (2016). 3 or 3'-Galloyl substitution plays an important role in association of catechins and theaflavins with porcine pancreatic  $\alpha$ -amylase: the kinetics of inhibition of  $\alpha$ -amylase by tea polyphenols. *Journal of Functional Foods*, 26, 144-156. <http://dx.doi.org/10.1016/j.jff.2016.07.012>.
- Udeh, B. A., & Erkurt, E. A. (2017). Compositional and structural changes in phoenix canariensis and opuntia ficus-indica with pretreatment: effects on enzymatic hydrolysis and second generation ethanol production. *Bioresource Technology*, 224, 702-707. <http://dx.doi.org/10.1016/j.biortech.2016.11.015>. PMID:27847237.
- Wang, J. Y., Gu, C. F., Ma, T. H., & Wang, R. (2022). Effects of foliar iron spraying on Cabernet Sauvignon phenolic acids and proanthocyanidins. *Food Science and Technology (Campinas)*, 42, e44622. <http://dx.doi.org/10.1590/fst.44622>.
- Wang, S. T., Zhuo, W. T., Dan, Y. Q., Qin, Z., Zhang, C. X., Xi, J., Liu, H. M., Ma, Y. X., & Wang, W. D. (2021). Inhibitory effects of Chinese quince fruit proanthocyanidins with different polymerisation degrees on the formation of heterocyclic aromatic amines in chemical model systems. *International Journal of Food Science & Technology*, 57(1), 330-341. <http://dx.doi.org/10.1111/ijfs.15409>.
- Wang, T., Jonsdottir, R., Liu, H. Y., Gu, L., Kristinsson, H. G., Raghavan, S., & Ólafsdóttir, G. (2012). Antioxidant capacities of phlorotannins extracted from the brown algae *Fucus vesiculosus*. *Journal of Agricultural and Food Chemistry*, 60(23), 5874-5883. <http://dx.doi.org/10.1021/jf3003653>. PMID:22612266.
- Waterlot, A. A., Le Bourvellec, C., Imbert, A., & Renard, C. M. G. C. (2014). Neutral sugar side chains of pectins limit interactions with procyanidins. *Carbohydrate Polymers*, 99(1), 527-536. <http://dx.doi.org/10.1016/j.carbpol.2013.08.094>. PMID:24274539.
- Wen, K. S., Ruan, X., Wang, J., Yang, L., Wei, F., Zhao, Y. X., & Wang, Q. (2019). Optimizing nucleophilic depolymerization of proanthocyanidins in grape seeds to dimeric proanthocyanidin B1 or B2. *Journal of Agricultural and Food Chemistry*, 67(21), 5978-5988. <http://dx.doi.org/10.1021/acs.jafc.9b01188>. PMID:31070025.
- Wojdyło, A., Nowicka, P., & Bąbelewski, P. (2018). Phenolic and carotenoid profile of new goji cultivars and their anti-hyperglycemic, anti-aging and antioxidant properties. *Journal of Functional Foods*, 48, 632-642. <http://dx.doi.org/10.1016/j.jff.2018.07.061>.
- Yang, N., Li, T., Ma, L., Sun, D., Jiang, Z., & Hou, J. (2019a). Characterization and structure of cold-extruded whey protein isolate: impact of ball milling. *Applied Nanoscience*, 9(3), 423-433. <http://dx.doi.org/10.1007/s13204-018-0913-7>.
- Yang, T., Dong, M. Q., Cui, J. Q., Gan, L., & Han, S. J. (2019b). Exploring and comparing two means of preparing and fractionating oligomeric proanthocyanidins from mangosteen pericarp: gel filtration chromatography and progressive solvent precipitation. *Analytical and Bioanalytical Chemistry*, 411(21), 5455-5464. <http://dx.doi.org/10.1007/s00216-019-01919-7>. PMID:31227847.
- Zeller, W. E. (2019). Activity, purification, and analysis of condensed tannins: current state of affairs and future endeavors. *Crop Science*, 59(3), 886-904. <http://dx.doi.org/10.2135/cropsci2018.05.0323>.
- Zhang, A. B., Li, J. J., Zhang, S. F., Mu, Y. B., Zhang, W., & Li, J. Z. (2017). Characterization and acid-catalysed depolymerization of condensed tannins derived from larch bark. *RSC Advances*, 7(56), 35135-35146. <http://dx.doi.org/10.1039/C7RA03410E>.
- Zhang, Y., Zhou, X., Tao, W., Li, L., Wei, C., Duan, J., Chen, S., & Ye, X. (2016). Antioxidant and antiproliferative activities of proanthocyanidins from Chinese bayberry (*Myrica rubra* Sieb. et Zucc.) leaves. *Journal of Functional Foods*, 27, 645-654. <http://dx.doi.org/10.1016/j.jff.2016.10.004>.